SYNTHESIS AND CHARACTERIZATION OF NIOBIUM AND TUNGSTEN SUBSTITUTED VOPO₄

SUBRATA CHANDRA ROY*, LILUFER YEASMIN AND MAHMUDUR RAHMAN

*Department of Chemistry, Jagannath University, Dhaka-1100, Bangladesh*

ABSTRACT

Tungsten and Niobium substituted α_{II}-VOPO₄ structure type solid solution $(V_{1-x-y}W_xNb_y)$ OPO₄ where $x = 0.07$ and $y \leq 0.05$ was synthesized by solution combustion technique followed by heating in air at 700˚C for 3 days. Further incorporation of niobium ($y > 0.05$) leads to a mixture of α_{II}-VOPO₄ structure type solid solution and two very weak reflections of another unknown phase. The synthesized product was characterized by X-ray powder diffraction, SEM/EDX, FTIR, and magnetic property analysis.

**Keywords:** solid solution, heterogeneous catalyst, x-ray powder diffraction

INTRODUCTION

For the period of last decades Vanadyl pyrophosphate, $(VO)_2P_2O_7$ (VPP) has been comprehensively studied due to its exceptional catalytic properties for the selective oxidation of *n*-butane to maleic anhydride (MA, furan-2,5-dione) (Borde*s et al.* 1979 and Schlögl 2009, eq. 1). The importance of MA can well be understood by its huge annual production of 2.7 million tons (Trifiro *et al.* 2014). The catalytic behavior of VPP is attributed to its exceptional physicochemical properties and crystal structure (Fig. 1).

$$n\text{-}C_4H_{10} + 7/2\,O_2 \xrightarrow{\text{VPP}} C_2H_2(CO)_2O + 4\,H_2O;$$
$$\Delta H = -1236\,KJ/mol \qquad \text{(eq. 1)}$$
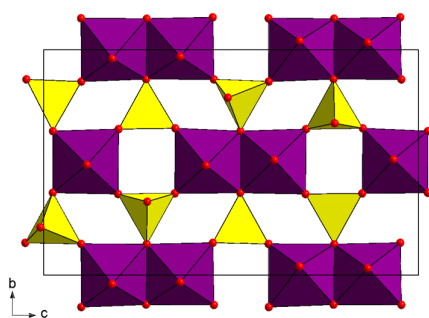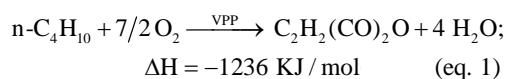
Fig. 1. Crystal structure of $(VO)_2P_2O_7$ (Hiroi *et al.*1999), deep V_2O_{10} edge-sharing dioctahedra, light P_2O_7 groups.

*Corresponding author: <scroy1979@yahoo.com>.

The true chemical composition and the structural properties of the active site of VPP for this catalytic reaction under operando conditions are still under debate (Hutching *et al.* 1998 and Hodnett 2000). Scientists are trying to explore the mystery of this complicated catalytic reaction process. However, this catalyst shows a conversion and yield of about 85% and 65% (Ballarini 2006), respectively. It was shown that an amorphous surface layer on crystalline $(VO)_2P_2O_7$ might be the active phase (Zazhigalov 1983). The existence of other polymorphs (α_{II}-, β-, γ-, δ-, ω-) of V^VOPO₄ were also confirmed by in-situ spectroscopic and diffraction studies (Hutching *et al.* 1994, Hutching *et al.* 1996, and Conte *et al.* 2006) This can be attributed to the oxidation of VPP as shown in eq. 2.

$$(VO)_2\,P_2O_7 + 0.5\,O_2 \rightarrow 2\,VOPO_4 \quad \text{(eq. 2)}$$
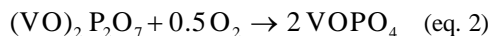
Scientists are yet to modify the existing catalyst by adding promoters or dopants, since there is enough opportunity to improve the yield of MA. However, studies on incorporation of catalytic promoters did not lead to an improved catalyst activity and selectivity (Agaskar *et al.* 1997, Davis *et al.* 2002, Guliants *et al.* 1999, Rownaghi *et al.* 2009). Recently it was reported that the catalytic activity and selectivity of various, polynaryvanadium (IV) phosphates

containing a transition metal (Cr, Fe, Ni, Cu) in the phosphate framework do not reach the conventional VPP catalyst (Glaum *et al.* 2007 and Benser *et al.* 2007).
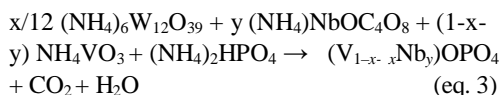
P. K. Grasselli (2002) reported that redox active transition metals with oxidation states are vanadium (IV, V), iron (II, III), copper (I, II), manganese (III, IV), molybdenum (V, VI), and rhenium (IV, V, VI, VII), niobium (IV, V) which could be potential components of oxidation catalyst materials. Aiming at the inclusion of mixed-valency in α_{II}-VOPO$_4$ by solid solution formation with $(V^{IV}O)Mo^{VI}O_4$ or $(Mo^VO)PO_4$ led to 7% of heterovalent substitution of PO$_4$ by MoO$_4$ and V^{5+} by V^{4+} (Raminosona *et al.* 1987). On the other hand, substitution of "Nb" by "W" in α-NbOPO$_4$, S.G. *P4/n* (Longo *et al.* 1996) lead to $(Nb^V_{0.787}W^V_{0.213})OPO_4$, S.G. *P4/nmm* (Leclaire *et al.* 1997) which is very much related to the host structure. It is worth to be mentioned that the high temperature polymorph β-NbOPO$_4$ (Leclaire *et al.* 1986) is isotypic to WOPO$_4$ (Wang *et al.* 1989, and Roy *et al.* 2016). However, information on solid solution formation among VOPO$_4$ NbOPO$_4$ and WOPO$_4$ were lacking in literature. This might be attributed to their different crystal structures and the quite different redox behavior of V^{5+}, Nb^{5+} and W^{5+}.

Here the synthesis and characterization of solid solution of polynaryphosphate, $(V_{1-x-y}W_xNb_y)$ OPO$_4$ (α_{II}-VOPO$_4$ type); where $x = 0.07$ and $0 \leq y \leq 0.15$ is reported. This solid solution allows to incorporation of a third redox active transition metal center "Nb" besides "V" and "W". α_{II}-VOPO$_4$ structure could be stabilized by substitution of vanadium by tungsten in the range of $0.04 \leq x \leq 0.24$ (Roy *et al.* 2014). Moreover, partial substitution of "V" by "W" in α_{II}-VOPO$_4$ leads to promising catalyst material for butane based oxidation (Schulz *et al.* 2018). Therefore to attain the α_{II}-VOPO$_4$ structure type solid solution the amount of "W" in the aiming product is taken 0.07.

MATERIALS AND METHODS

Synthesis of solid solution of polynaryphosphates.

The aimed α_{II}-VOPO$_4$ structure type solid solution of polynaryphosphates, $(V_{1-x-y}W_xNb_y)OPO_4$ where $x = 0.07$ and $0 \leq y \leq 0.15$ were synthesized by solution combustion synthesis, SCS (Patil *et al.* 1997 and Moore *et al.* 1995) followed by heating the reaction intermediates after combustion in air up to 700 °C according to eq. 3.

$$x/12\ (NH_4)_6W_{12}O_{39} + y\ (NH_4)NbOC_4O_8 + (1-x-y)\ NH_4VO_3 + (NH_4)_2HPO_4 \rightarrow (V_{1-x-x}Nb_y)OPO_4 + CO_2 + H_2O \qquad (eq.\ 3)$$

Appropriate amount of precursor materials: ammonium metatungstate $[(NH_4)_6W_{12}O_{39}$ 5.21H$_2$O], ammonium niobate(V) oxalate $[(NH_4)$ NbOC$_4$O$_8\cdot$0.59H$_2$O], diammonium hydrogen phosphate $[(NH_4)_2HPO_4]$, and ammonium metavanadate $[(NH_4)VO_3]$ (all from Sigma Aldrich, p.a) were dissolved in minimum amount of water together with oxidizer (HNO$_3$) and fuel (glycine) with continuous stirring as described in Roy *et al.* 2014.

X-ray powder Diffraction analysis

The X-ray powder patterns of the samples $(V_{1-x-y}W_xNb_y)$ OPO$_4$ were taken by Rigaku Ultima IV diffractometer at the Centre for Advanced Research Centre, (CARS) University of Dhaka, Bangladesh. The operating conditions of the diffractometer were 40 kV, 40 mA, Cu-Kα_1 radiation ($\lambda = 1.54051$ $^{\mathring{o}}$), exposure time 3 deg/minute.

SEM and EDX analysis

Scanning Electron Microscopic and Energy Dispersive X-ray analysis were carried out by Zeiss Evo 18 (operated at 10 kV) and EDAX, respectively from Bangladesh Council of Science and Industrial Research (BCSIR), Dhaka-1205, Bangladesh. The sample was sputtered with gold before EDX analysis and three different areas of the sample were focused with electron beam to get the average elemental composition.

Magnetic measurements

The mass magnetic susceptibility of the powder sample was measured by magnetic susceptibility balance MARK 1, (Sherwood Scientific Ltd., Cambridge) at Jagannath University, Dhaka-1100, Bangladesh using the eq. 4.

$$X_g = C. \frac{l}{m}. \frac{(R-R_0)}{10^9} \qquad \text{(eq. 4)}$$

Where, l = 3cm (length of sample on sample holder); m = 0.241 g, mass of the sample; $(R-R_0)$ = 7-(-29), difference between balance reading for the sample holder tube with sample and without sample; C=957.08×10^{-6}, proportionality constant.

FTIR analysis

The FTIR analysis was carried out by Shimadzu IR Tracer-100 at Jagannath University, Dhaka-1100, Bangladesh. The powder sample was mixed and ground with highly purified KBr (p.a.) as approximate 10:1 ratio in a clean agate mortar to a fine powder. Transparent discs from that mixture were prepared by manual pressing. All the infrared transmission spectra were determined at room temperature in the range of wave number 400 to 4000 cm^{-1}.

RESULTS AND DISCUSSION

X-ray powder diffraction patterns of powder samples show single-phase solid solution $(V_{1-x\,y}W_xNb_y)OPO_4$ where $x = 0.07$ and $0.0 \leq y \leq 0.05$ with α_{II}-VOPO$_4$ structure type (Fig. 2.). Further incorporation of niobium $0.05 < y \leq 0.15$ leads to two very weak diffraction peaks of unknown phase. With increasing the niobium concentration the intensity of unknown phase increases but it is very little. Due to small number of diffraction peaks as well very low intensity, they are not possible to index.
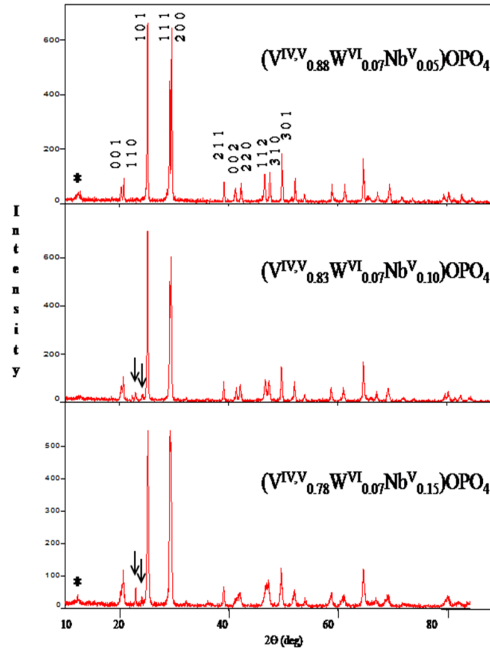
Fig. 2. Comparison of X-ray powder diffraction patterns of members of the solid solutions $(V_{1-x-y}W_xNb_y)$ OPO$_4$ (with $x = 0.07$ and $0.0 \leq y \leq 0.15$) where $0.0 \leq y \leq 0.05$ is only α_{II}-VOPO$_4$ structure type, and y> 0.05 is mixture α_{II}-VOPO$_4$ structure type solid solution and an unknown phase (indicated by down arrows). Asterisks are VOPO$_4$·2H$_2$O type phase due to hydration of $(V_{0.88}W_{0.07}Nb_{0.05})OPO_4$ in lab condition.

Exposure of solid solution $(V_{1-x-y}W_xNb_y)$ OPO$_4$, with α_{II}-VOPO$_4$ structure type to lab atmosphere over a period of several days led to their hydration, as it is suggested by the XRPD pattern of the phases (Fig. 2., indicated by asterisk), which is very similar to the one observed for $(V_{1-x}W_x)$ OPO$_4$·2H$_2$O and VOPO$_4$·2H$_2$O (Roy *et al.* 2014, and Tietze 1981). The layer type structure of $(V_{0.88}W_{0.07}Nb_{0.05})$ OPO$_4$ (α_{II}-VOPO$_4$ structure type, (Fig. 3) allows the incorporation of water molecules as guest species between the layers of the host structure.
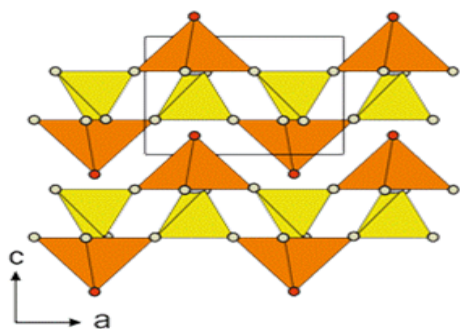
Fig. 3. Polyhedral representation of $(V_{0.88}W_{0.07}Nb_{0.05})OPO_4$ (α_{II}-VOPO$_4$ type). [MO$_5$] square pyramids (M = V/W/Nb): deep, [PO$_4$] tetrahedra: light, filled circles represent oxygen atoms of (M=O)$^{3+}$.

Immediately after ignition at 400°C for five minutes the XRPD pattern of the combustion product shows reflections of Keggin type structure, $(NH_4)_3PW_{12}O_{40}\cdot 9.5\ H_2O$ (Zubkov 1998) as shown in Fig. 4. Further heating (stepwise upto 600°C) of the material after grinding in an agate mortar shows the same phase. The aimed solid solution $(V_{0.88}W_{0.07}Nb_{0.05})OPO_4$ is obtained at 700°C for 3 days.

The formation of Keggin type structure, $(NH_4)_3PW_{12}O_{40}\cdot 9.5\ H_2O$ prior to the occurrence of aimed solid solution, $(V_{0.88}W_{0.07}Nb_{0.05})OPO_4$ (α_{II}-VOPO$_4$ structure type) is obvious.

IR spectrum Fig. 5 shows that a weak peak at 1091 cm^{-1} which corresponds to the asymmetric stretching vibration of the PO$_4$ tetrahedra, while the peak at 921 cm^{-1} can be assigned to the symmetric stretching vibration of the PO$_4$ tetrahedra (R'kha *et al.* 1986). In addition, the peaks at 534 cm^{-1} and 427 cm^{-1} reflect the bending vibration of the PO$_4$ tetrahedra. Symmetric stretching mode of M=O (M: V/Nb/W) of vanadyl group was observed at 968 cm^{-1} (Barraclough *et al.* 1959). Furthermore, the sharp peaks close to 605, and 628 cm^{-1} can be
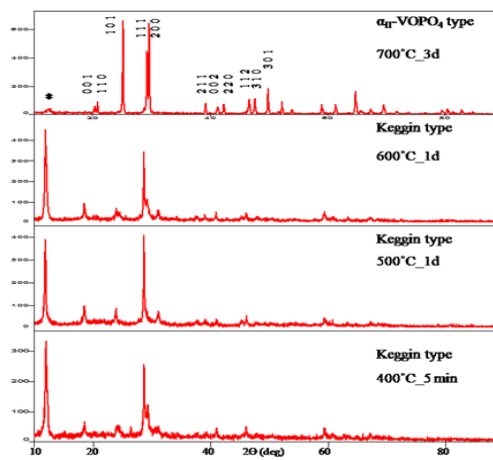
Fig. 4. Powder diffraction patterns $(V_{0.88}W_{0.07}Nb_{0.05})OPO_4$, showing the progress of phase formation with temperature by heating in air. Asterisks are VOPO$_4\cdot 2H_2O$ type due to hydration of $(V_{0.88}W_{0.07}Nb_{0.05})OPO_4$ in lab condition.

attributed to the M-O bending vibrations in MO$_6$ octahedra. The weak and broad band at 3527 and 1635 cm^{-1} arises from the O-H bond stretching modes and HOH bending modes, respectively. Weak band at 686 cm^{-1} corresponds to bending vibration modes of (M-OH) or (P-OH). The incorporation of water molecule is also confirmed by XRPD (Fig. 2.) as hydration of $(V_{0.88}W_{0.07}Nb_{0.05})OPO_4$ led to formation of $(V_{0.88}W_{0.07}Nb_{0.05})OPO_4\cdot 2H_2O$.

The magnetic measurement of the powder sample of $(V_{0.88}W_{0.07}Nb_{0.05})OPO_4$ reveals the paramagnetic behavior. The measured mass susceptibility, χ_g (at room temperature, 28°C) is 428.90×10^{-9} cm^3 g^{-1} and the molar magnetic susceptibility, χ_{mol} is 112.41×10^{-6} cm^3 mol^{-1}. Roy *et al.* reported (2014) that incorporation of W^{6+} in α_{II}-V^{V}OPO$_4$ led reduction of V^{5+} to V^{4+} according to $(V^{IV}_{0.24}V^V_{0.52}W^{VI}_{0.24})OPO_4$. Therefore, paramagnetic property of $(V_{0.88}W_{0.07}Nb_{0.05})OPO_4$ can be attributed to the presence of tetravalent vanadium as $(V^{IV}_{0.07}V^V_{0.81}W^{VI}_{0.07}Nb^V_{0.05})OPO_4.$
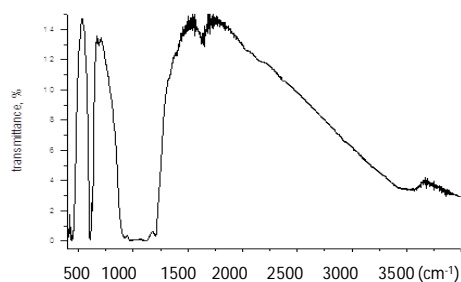
Fig. 5. FTIR spectrum of solid solution $(V_{0.88}W_{0.07}Nb_{0.05})OPO_4$ (α_{II}-VOPO$_4$ type) with KBr.

The SEM image of $(V_{0.88}W_{0.07}Nb_{0.05})OPO_4$ (Fig. 6a) shows crystallites with homogeneous morphology which indicates all the crystallites contain same type of elements. The EDX result shows no hints on impurity elements (Fig. 6b) and the average atomic (%) ratio of V:W:Nb:P = 46.1:2.4:2.0:49.5 which is close to the nominal composition 44.0:3.5:2.5:50.0, respectively.
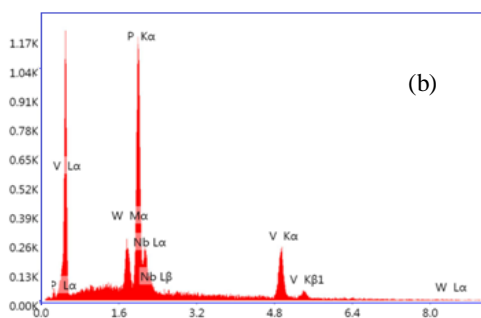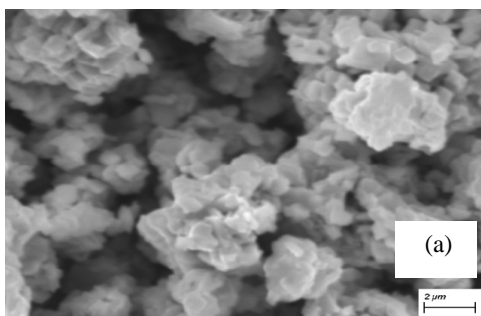
Fig. 6. SEM image (a), and EDX spectrum (b), of $(V_{0.88}W_{0.07}Nb_{0.05})$ OPO$_4$.

CONCLUSION

Pure VOPO$_4$ is catalytically dead for the partial oxidation of n-butane to maleic anhydride however, only tungsten substituted VOPO$_4$, $(V_{1-x}W_x)OPO_4$; where $0 \leq x \leq 0.24$ (α_{II}-VOPO$_4$ structure type) [Schulz *et al.* 2018] leads to a new catalyst material for that purpose. Since the insertion of another redox active transition metal, niobium in presence of tungsten might increase this catalytic efficiency. Therefore, the niobium and tungsten substituted α_{II}-VOPO$_4$ type solid solution $(V_{1-x-y}W_xNb_y)$ OPO$_4$; where x=0.07 and $y \leq 0.05$ (α_{II}-VOPO$_4$ structure type) was synthesized by solution combustion technique followed by heating in air at 700˚C for 3 days. The metanyl bond (M = O; M: V, Nb, W) and bonds in PO$_4$ were confirmed by FTIR spectrum. The paramagnetic behavior of the synthesized product indicates the presence of tetravalent vanadium and EDX analysis showed the incorporation of both tungsten and niobium in α_{II}-VOPO$_4$ structure type phase.

REFERENCES

Agaskar P. A., P. K. Grasselli, D. J. Buttrey and B. White. 1997. Structural and catalytic aspects of some NASICON - based mixed metal phosphates, *Stud. Surf. Sci. Catal.*, **110**: 219-226.

Ballarini N., F. Cavani, C. Cortelli, S. Ligi, F. Pierelli, F. Trifiro, C. Fumagalli, G. Mazzoni and T. Monti. 2006. VPO catalyst for *n*-butane oxidation to maleic anhydride: A goal achieved, or a still open challenge? *Top. Catal.* **38**: 147-156.

Barraclough C. G., J. Lewis, and R. S. Nyholm. 1959. The stretching frequencies of metal–oxygen double bonds, *J. Chem. Soc.*, p3552-3555.

Bordes E. and P. Courtine. 1979. Some selectivity criteria in mild oxidation catalysis: VPO phases in butene oxidation to maleic anhydride, *J. Catal* **57**: 236-252.

Conte M., G. Budroni, J. K. Bartley, S. H. Taylor, A. F. Carley, A. Schmidt, D. M. Murphy, F. Girgsdies, T. Ressler, R. Schlögl and G. J. Hutchings. 2006. Chemically Induced Fast Solid-State Transitions of ω-$VOPO_4$ in Vanadium Phosphate Catalysts, *Science* **313**: 1270-1273.

Davis M. E., C. J. Dillon, J. H. Holles and J. Labinger. 2002. A New Catalyst for the Selective Oxidation of Butane and Propane, *Angew. Chem. Int. Ed.*, **41**: 858-860.

Glaum R., E. Benser and H. Hibst. 2007. Novell Ternary and Polynary Vanadium (IV) Phosphates as Catalysts for Selective Oxidations of Light Hydro-carbons, *Chem. Ing. Tech* **79**: 843-850

Grasselli P. K., 2002, Fundamental Principles of Selective Heterogeneous Oxida-tion Catalysis, *Top. Catal.*, **21**:79-88.

Guliants V. V, J. B. Benziger, S. Sundaresan, I. E. Wachs and A. M. Hirt. 1999. *Cat. Lett.*, **62**: 87-91.

Hiroi Z, M. Azuma, Y. Fujishiro, T. Saito, M. Takano, F. Izumi, T. Kamiyama and T. Ikeda. 1999. Structural Study of the Quantum-Spin Chain Compound $(VO)_2P_2O_7$, *J. Solid State Chem.*, **146**: 369-379.

Hodnett B. K. 2000. *Heterogeneous Catalytic Oxidation*, John Wiley & Sons, Chichester.

Hutchings G. J., A. Desmartin-Chomel, R. Oller and G. J. Volta. 1994, Role of the product in the transformation of a catalyst to its active state, *Nature*, **368**: 41-45.

Hutchings G. J., C. J. Kiely, M. T. S. Schulz, A. Burrows and J.-C. Volta. 1998. Comments on the nature of the active site of vanadium phosphate catalysts for butane oxidation, *Catal. Today*, **40**: 273-286.

Hutchings G. J., I. J. Ellison, M. T. Sananes and J.-C. Volta 1996, *Catal. Lett.* **38**: 231-237.

Leclaire A., M. M. Borel and B. Raveau. 1997. Combination of α-$NbOPO_4$ type layers with enantiomorphic α′-type layers: the "racemic structure" of α-α′-$Nb_{0.787}W_{0.213}OPO_4$, *Z. Kristallogr.*, **212**: 837-839 .

Leclaire A., H. Chahboun, D. Groult and B. Raveau. 1986. The crystal structure of ß-$NbPO_5$, *Z. Kristallogr.* **177**: 277-286.

Longo J. M. and P. Kierkegaard. 1966. The crystal structure of $NbOPO_4$, *Acta Chem. Scand.* **20**: 72-78.

Moore J. J. and H. J. Feng. 1995. Combustion synthesis of advanced materials: Part I. Reaction parameters**,** *Prog. Mater. Sci.*, **39**: 243-273.

Moore J. J. and H. J. Feng. 1995. Combustion synthesis of advanced materials: Part II. Classification, applications and modeling, *Prog. Mater. Sci.* **39**: 275-316.

Patil K. C., S. T. Aruna and S. Ekambaram. 1997. Combustion Synthesis, *Current Opinion Sol. St. Mat. Sci.*, **2**. 158-165.

Raminosona A., E. Bordes and P. Courtine. 1987. Molybdenum-doped V-P-O system: I. Preparation and characteri-zation, *J. Solid State Chem.*, **68**: 1-10.

R'Kha C., M. T. Vandenborre and J. Livage. 1986, Spectroscopic study of colloidal $VOPO_4 \cdot 2H_2O$, *J. Solid State Chem.*, **63**: 202-215.

Rownaghi A. A., Y. H. T. Yap and F. Rezaei. 2009. Influence of rare-earth and bimetallic promoters on various VPO catalysts for partial oxidation of n-butane, *Cat. Lett*, **130**: 504-516.

Roy S. C., W. Assenmacher, T. Linden, L. Esser, W. Mader and R. Glaum. 2016. Substitution of W^{5+} in Monophosphate Tungsten Bronzes by Combinations M^{n+}/W^{6+}, Z. für Naturforschung B **71**: 543-552.

Roy S. C., R. Glaum, D. Abdullin, O. Schiemann, N. Q. Bac and K-W. Lii. 2014. Solid Solution Formation between Vanadium(V) and Tungsten(V) Oxide Phosphate, *Z. Anorg. Allg. Chem.*, **640**: 1876-1885.

Schlögl R., 2009, *Modern Heterogenous Oxidation Catalysis* (Ed: N. Mizuno), Wiley VCH, Weinheim.

Schulz C., S. C. Roy, K .Wittich, R. N. d'Alnoncourt, S. Linke, V. Strempel. B. Frank, R. Glaum and F. Rosowski. 2018. α_{II}-(V$_{1-x}$W$_x$)OPO$_4$ catalysts for the selective oxidation of *n*-butane to maleic anhydride, *Catal. Today*, *in press*, https: //doi.org/10. 1016/j.cattod. **2018**.05.040.

Tietze H. R., 1981. The crystal and molecular structure of oxovanadium (V) orthophosphate dihydrate, VOPO$_4\cdot$2H$_2$O *Aus. J. Chem.* s**34**: 2035-2038.

Trifiro F. and P. K. Grasselli. 2014. How the Yield of Maleic Anhydride in n-Butane Oxidation, Using VPO Catalysts, was Improved Over the Years, *Top. Catal.*, **57**: 1188-1195.

Wang S.-L., C.-C. Wang and K.-H. Lii. 1989. Crystal structure of WPO$_5$, the second member of the monophosphate tungsten bronze series (WO$_3$)$_{2m}$(PO$_2$)$_4$, *J. Solid State Chem.*, **82**: 298-302.

Zazhigalov V. A., A. I. Pyatnitskaya, I. V. Bacherikova, G. A. Komashko, G. Ladwig and V. M. Belousov. 1983. Dependence of the activity of vanadium-phosphorus catalysts on the V^{4+}/V^{5+} ratio in oxidation of butane, *React. Kinet. Catal. Lett.* **23**: 119-123.

Zubkov V., 1998. Inst. of Solid State Chemistry, Ekaterinburg, Russia, ICDD Grant-in-Aid, Powder Diffraction File-2.

(Received revised manuscript on 21 April 2019)